



2

## FOREIGN TECHNOLOGY DIVISION

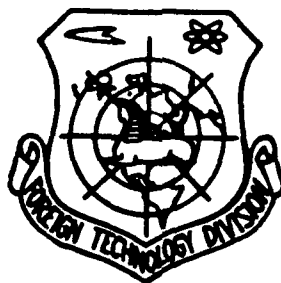


APPLICATIONS OF HOLOGRAPHIC LENSES IN HEAD UP DISPLAYS

by

Chen Huangming, Lu Bo

DTIC  
ELECTE  
AUG 09 1991  
S B D



Approved for public release;  
Distribution unlimited.

64

91-07194



91 8 27 064

## HUMAN TRANSLATION

FTD-ID(RS)T-0166-91

5 June 1991

MICROFICHE NR: FTD-91-C-000414

APPLICATIONS OF HOLOGRAPHIC LENSES IN HEAD UP DISPLAYS

By: Chen Huangming, Lu Bo

English pages: 17

Source: Yingyong Jiguang, Vol. 6, Nr. 5, 1986,  
pp. 223-228

Country of origin: China

Translated by: SCITRAN

F33657-84-D-0165

Requester: FTD/TTTRL/Lisa Tidd

Approved for public release; Distribution unlimited.

THIS TRANSLATION IS A RENDITION OF THE ORIGINAL FOREIGN TEXT WITHOUT ANY ANALYTICAL OR EDITORIAL COMMENT. STATEMENTS OR THEORIES ADVOCATED OR IMPLIED ARE THOSE OF THE SOURCE AND DO NOT NECESSARILY REFLECT THE POSITION OR OPINION OF THE FOREIGN TECHNOLOGY DIVISION

PREPARED BY:

TRANSLATION DIVISION  
FOREIGN TECHNOLOGY DIVISION  
WPAFB, OHIO

# GRAPHICS DISCLAIMER

All figures, graphics, tables, equations, etc. merged into this translation were extracted from the best quality copy available.



<b>Accession For</b>	
NTIS GRA&I	<input checked="" type="checkbox"/>
DTIC TAB	<input type="checkbox"/>
Unannounced	<input type="checkbox"/>
Justification	
By	
Distribution/	
Availability Codes	
Dist	Avail and/or Special
A-1	

**TITLE:** APPLICATIONS OF HOLOGRAPHIC LENSES IN HEAD UP DISPLAYS  
**AUTHOR:** Chen Huangming, Lu Bo

**SUMMARY** This article does research on the formation of images and aberration characteristics associated with holographic lenses, and brings out the design principles, design programs, and actual examples for holographic head up display devices.

Head up displays are one type of advanced observation and aiming instrument which is used in modern aircraft--in particular, in fighter planes. They are capable of supplying to flight personnel a wealth of flight information, and they have great significance for lightening the observation burden on flight personnel and raising the combat characteristics of the aircraft. As far as the important sections in the optical systems of head up displays are concerned, although they normally possess the strong points of familiarity of the industrial techniques in their manufacture, and simplicity and ease of structural installation; however, due to such weak points as small field of vision and the contradiction between high transparency and high reflection, very great limitations have been placed on the exerting of the capabilities of head up display devices. However, holographic lenses are still capable of very satisfactorily resolving these two problems. Because of this, one has seen the appearance of taking holographic lenses and replacing the holograph type optical systems of composite devices. This article will make a simple introduction of our most recent work in this area.

#### THE PRINCIPLES AND SPECIAL FEATURES OF HOLOGRAPHIC LENS IMAGE FORMATION

Holographic lenses are a type of image forming component based on the foundation of the theory of optical diffraction. The principle of its image formation is capable of being used in the form described below (Fig.1).

One takes  $OO$  and  $OR$  and, respectively, designates them as being the axis of light (optical axis) for the object and the axis of light for the image. The stipulations for the symbols  $d_O$  and  $d_R$  are as follows: they take the coordinate origin as starting point and go to the recorded light source, the direction of propagation of the unhindered light rays is positive, those in the opposite direction are

negative.

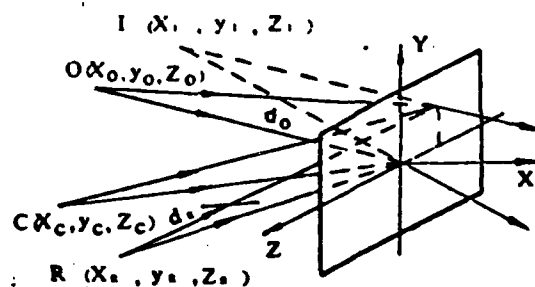


Fig.1 Principles of Image Formation in Holographic Lenses

$$\begin{cases} \frac{1}{d_i} = \frac{1}{d_c} + \mu \left( \frac{1}{d_o} - \frac{1}{d_R} \right) \\ \frac{y_i}{d_i} = \frac{y_c}{d_c} + \mu \left( \frac{y_c}{d_o} - \frac{y_R}{d_R} \right) \\ \frac{z_i}{d_i} = \frac{z_c}{d_c} + \mu \left( \frac{z_c}{d_o} - \frac{z_R}{d_R} \right) \end{cases} \quad (1)$$

The definition of the reciprocal of the focal distance or length of holographic lenses is:

224

$$\frac{1}{f'} = \mu \left( \frac{1}{d_o} - \frac{1}{d_R} \right) \quad (2)$$

When the object is located at an infinite distance, the equations for the relationships corresponding to image formation are:

$$\begin{aligned} \cos \beta_i &= \cos \beta_o + \mu (\cos \beta_o - \cos \beta_R) \\ \cos \gamma_i &= \cos \gamma_o + \mu (\cos \gamma_o - \cos \gamma_R) \end{aligned} \quad (3)$$

The stipulations for the symbols  $\cos \beta_I$  and  $\cos \gamma_I$  are that included angles between the direction of light propagation and the positive direction of the coordinate axes, which are smaller than  $90^\circ$ , are positive.

Employed in holographic head up displays are reflective type holographic lenses. They are capable of being seen as a composite body of a simple lens, a raster or grating, and reflective lenses possessing different media layers.

#### DISTRIBUTION OF HOLOGRAPHIC LENS FOCAL SURFACES AND SPECIFICATION OF IDEAL IMAGE SURFACES

The formula for the focal distance of holographic lenses is determined in Fresnel approximation. Fresnel approximation, besides being able to satisfy the condition that  $d_0$  and other similar quantities be sufficiently large, also has a condition which is that the range of values from which  $y$  and  $z$  are selected not be too large. In actual fact, holographic lens aperture diameters are always on a level at an order of magnitude with  $d_0$  and  $d_R$  or an order of magnitude smaller. Because of this,  $d_0$  and  $d_R$  certainly cannot be as shown in Fig.1. They can only be seen as distances from the recorded light source to the origin point of the coordinates. Moreover, they should be seen as the distances from the recorded light sources to a certain point on the holographic lens. Following along with this, the differences in locations of these points are in process of change. As a result of this, the focal length  $f'$  is not a constant.

In order for us to analyze, under the recording conditions shown in Fig.2, the focal distribution status of the holographic lenses is:

$$f_s = \frac{DR \cdot DO}{DR - DO}, \quad f_n = \frac{DRH \cdot DOH}{DRH - DOH}$$

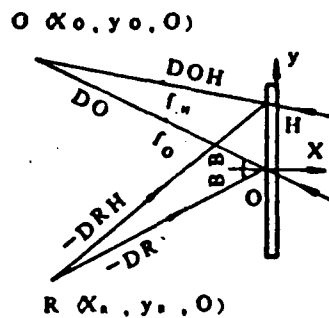


Fig.2 Focal Surface Analysis of Holographic Lens

In this,

$$\begin{aligned} DRH &= -\sqrt{DR^2 - 2DR \cdot \sin B \cdot H + H^2}, \\ DOH &= \sqrt{DO^2 - 2DO \cdot \sin B \cdot H + H^2}, \quad DO, DR, \\ &B \end{aligned}$$

which are determined at the time of recording.  $H$  is related to the light passage aperture diameter of the holographic lens required.

$$\begin{aligned} x_{fH} &= -\cos B \cdot \frac{|DR| \cdot DO}{|DR| + DO} \\ x_{fH} &= -DO \cdot \cos B \cdot \\ &\frac{\sqrt{DR^2 + 2 \cdot |DR| \cdot H \cdot \sin B + H^2}}{\sqrt{DR^2 + 2 \cdot |DR| \cdot H \cdot \sin B + H^2} + DOH} \end{aligned}$$

It is possible to see that  $x_{fH}$  is a complex function of  $H$ . It expresses the fact that the focal surfaces of holographic lenses are complex curved surfaces. If one will have  $x_{fH} \approx x_{f0}$ , it is not difficult to obtain:

$$H[H(DO - |DR|) + 2 DO \cdot |DR| \sin B] \leq 0$$

(4)

Going through an analysis of equation (4), it is possible to see the distribution of special points on this curved surface. When  $B = 0$ , we then have a situation in which common axes are recorded. From equation (4), one obtains:  $DO \leq |DR|$ . This clearly shows that, in this situation, whether or not  $x_{fH}$  is smaller than, equal to, or larger than  $x_{fO}$ , it is not related to  $H$ .

When  $DO > |DR|$ ,  $x_{fH} < x_{fO}$ . The focal surface of the holographic lens is a curved surface convex toward the holographic lens (Fig.3a).

When  $DO = |DR|$ ,  $x_{fH} = x_{fO}$ . The focal surface of the holographic lens is a planar surface perpendicular to the axis of the light (Fig.3b).

When  $DO < |DR|$ ,  $x_{fH} > x_{fO}$ . The focal surface of the holographic lens is a curved surface concave toward the holographic lens (Fig.3c).

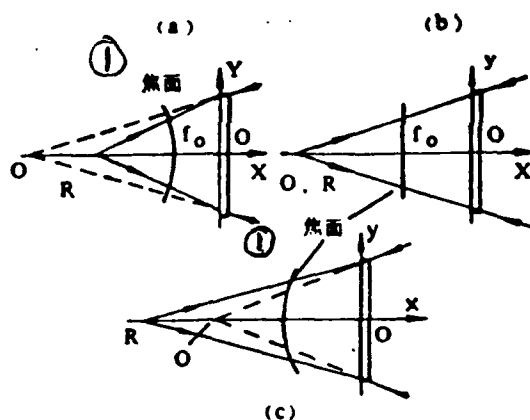


Fig.3 Focal Surface Distribution of Coaxial Holographic Lenses (1)  
Focal Surface



When  $B \neq 0$ , then one has a situation in which records are made away from the axes. From equation (4), and, in conjunction with that, on the basis of the range of selected values which it is possible to make use of for  $H$  in practical terms, it is possible to prove that it goes without saying  $DQ \leq |DR|$ . Also, one has: .  
 When  $H > 0$ ,  $x_{fH} < x_{f0}$ . When  $H = 0$ ,  $x_{fH} = x_{f0}$ . And, when  $H < 0$ ,  $x_{fH} > x_{f0}$ .

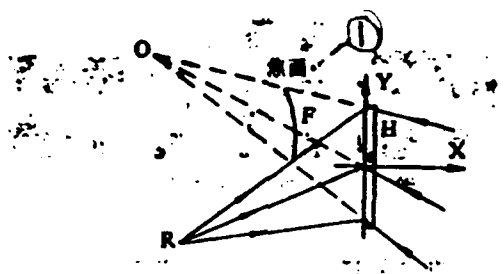


Fig.4 Focal Surface Distribution for Holographic Lenses Off the Axes  
 (1) Focal Surface

At this time, the focal surface distribution for holographic lenses is as shown in Fig.4.

On the basis of the analysis above, it is possible to come to the following conclusions.

In situations where one has coaxial recording, the focal surfaces of holographic lenses are distributed symmetrically with respect to the axis of the light. Under conditions of recording off the axes, focal surfaces are curved surfaces which are oblique with respect to the axis of the light. This distinction has led to extremely great differences between coaxial holographic lenses and holographic lenses off the axes with respect to image formation and aberration characteristics.

How, in the vicinity of focal surfaces, to select a planar surface to act as an ideal image surface for forming images from holographic lenses of objects at an infinite distance away is an extremely important question. This article recognizes that there are

two questions which should be considered:

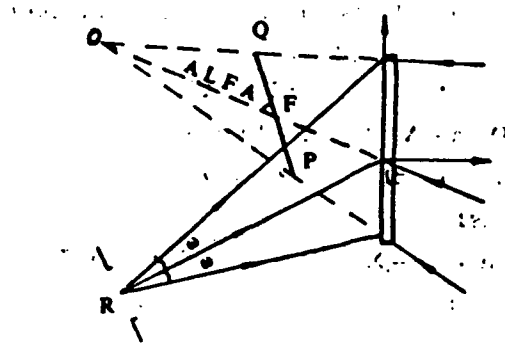


Fig.5 Precise Determination of Ideal Image Forming Surface for Holographic Lenses

1. This planar surface should cross the focal point F on the axis of the light, and one should do everything possible to follow the focal surface. This is advantageous to the balancing of aberrations (Fig.5).

2. As far as taking the focal point F as the point of symmetry in the center of the planar surface in question (for example, P and Q) is concerned, this should correspond and have the same vision field angle  $\omega$ .

On the basis of points P and Q corresponding to different fields of vision, it is possible to solve for a considerable number of planar image surfaces. On a certain planar image surface, there is only one set of symmetrical points corresponding to the same field of vision. Table 1 gives the distributions for these planar image surfaces in three types of situations. Table 2 gives the relationships between the planar image surface oblique angles  $ALFA$  and the angles off axes WJ. One can see that:

1. Under given recording conditions, the included angles between these planar image surfaces are very small. Because of this, it goes without saying that it is alright no matter which plane is selected to act as the ideal image surface.

2. Following along with increases in the angles off axes, the obliqueness of the planar image surfaces is every more severe, and ALFA is ever smaller.

DO = - DR = 500 WJ = 45° UJ = 67.5° ω = 11°					
ω	1	0.85	0.7	0.5	0.3
ALFA	50.361°	50.360°	50.362°	50.355°	50.382°
DO = - DR = 500 WJ = 45° UJ = 45° ω = 11°					
ω	1	0.85	0.7	0.5	0.3
ALFA	45°	45°	45°	45°	45°
DO = 800 DR = - 500 WJ = 45° UJ = 90° ω = 11°					
ω	1	0.85	0.7	0.5	0.3
ALFA	41.473°	41.473°	41.473°	41.474°	41.482°

Table 1

DO = DR = - 500 ω = 11°			
WJ	15°	30°	45°
ALFA	75.280°	61.894°	50.382°
WJ	60°	75°	90°
ALFA	40.914°	35.089°	26.565°

Table 2

## EXPERIMENTAL ANALYSIS OF IMAGE ABERRATION IN HOLOGRAPHIC LENSES

As far as a comparison of the special characteristics of image formation with holographic lenses and normal optical components is concerned, there are two key points which are the biggest distinctions between them: 1. the obliqueness of image surfaces, and 2. nonsymmetrical distributions of aberration.

Talking in terms of this type of nonsymmetrical image formation component in holographic lenses, when one is calculating aberration distributions for aberration light packets or bundles, one should not only calculate aberration distributions for the meridian direction of the object light packets forming the image. Moreover, one should calculate aberration distributions for the arc vector direction of the object light packets forming the image. The special point about the arc vector light packets from the object forming the image is that, after coplanar light rays radiating in go through holographic lenses, they are not necessarily coplanar. Because of this, when describing the special points associated with their aberration distributions, one uses the degree of diffusion or dispersion on image surfaces of image forming light packets in order to describe them.

226

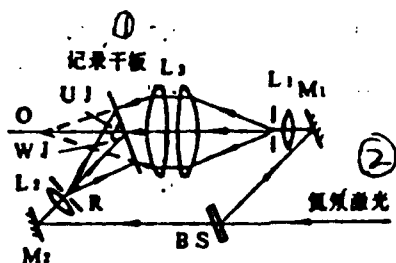


Fig.6 Record Light Path (1) Dry Recording Plate (2) Helium-Neon Laser

This article carried out experimentation and proved the light path as shown in Fig.6. In it,  $DO = -DO = 250$  mm.  $WJ = 45^\circ$ .  $UJ = 67.5^\circ$ . According to Fig.6, we made a focal length of 125 mm for a holographic lens with a light passing aperture diameter that was 45 mm. Silver salt dry plates from the Tianjin Photosensitive Film Plant were used in the tests. We opted for the use of D 19 development, F 5 fixative, potassium ferrocyanide bleaching, and used air drying with electric fans. We chose to use the light path shown in Fig.7 in order to observe the image point distribution of the holographic lenses and the status of aberration distributions on the axis. We directly used laser light to illuminate and cause reappearances. Due to the relative thinness of laser light bundles, speaking in terms of the holographic lenses, it is possible to see them as forming images out of the thin light bundles, going through position fixing markers, turning and reflecting at mirror M, and as being capable of supplying to the holographic lens image forming light bundles at an unlimited distance for different fields of view.

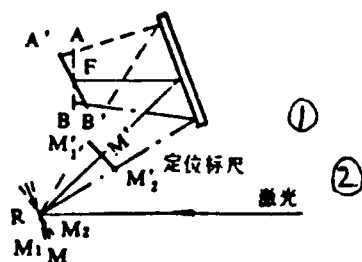


Fig.7 Observation Light Path (1) Position Fixing Marker (2) Laser Light

On the two surfaces of observation, we, respectively, carried out this experiment. One was on the surface AB perpendicular to the light axis of the image area. One was on the surface A'B', which this article defines as the ideal image surface. Fig.8 is the results of the experiments. In these, (b) is the experimental result for the ideal image surface as defined in this article. It is possible to see

that the image point distribution for (a) is not symmetrical. However, (b)'s image point distribution is symmetrical. This makes it clear that the method presented by this article for accurately fixing the ideal image surface for holographic lenses is correct. Fig.9 is the status of aberration distributions as recorded for thin light bundle image formation on axes, both before and after observed surfaces are moved. It is completely in line with the results of calculated analyses of aberrations.



Fig.8 Status of Image Point Distributions

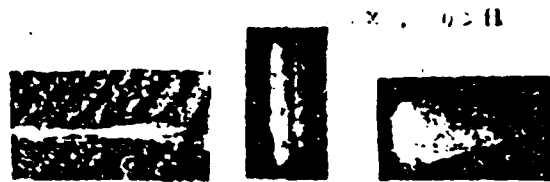


Fig.9 Status of Aberration Distributions on Axes

#### THE PURSUIT OF LIGHT PATHS IN NONCOAXIAL SYSTEMS WITH SPHERICAL SURFACES

Aberration calculations for noncoaxial systems with spherical surfaces are a very complicated problem. As far as the two situations of eccentricity and obliqueness in noncoaxial included spherical surfaces are concerned, for the situation of eccentricity, it is possible to induce one's way into the oblique situation. Normally, one only takes them to act as factors influencing the quality of image

formation in order to add to controls. However, very infrequently, one takes them to act as variables in the calibration of aberration in order to add to utilizations. However, in holographic optical systems, one must always make use of them in order to calibrate aberrations. This article derives accurate light path tracking formulae for the oblique case in the meridian planes of spherical surfaces:

$$\begin{aligned}
 a &= a(d - X) - \beta Y - v Z \\
 M_x &= X - d + a\alpha, \quad M_y = Y + a\beta \\
 M^2 &= M_x^2 + M_y^2 + (Z + av)^2 \\
 A &= a \cos \theta + \beta \sin \theta, \quad B = M_x \cos \theta + M_y \sin \theta \\
 \Delta &= \frac{M^2 C - 2 B}{A + \sqrt{A^2 - M^2 C^2 + 2 CB}} \\
 D &= a + \Delta, \quad X_1 = X - d + a D \\
 Y_1 &= Y + \beta D, \quad Z_1 = Z + v D \\
 \cos I &= |a(\cos \theta - X_1 C) + \beta(\sin \theta - Y_1 C) - v Z_1 C| \\
 \cos I' &= \sqrt{1 - n^2(1 - \cos^2 I)/(n')^2} \\
 g &= n' \cos I' - n \cos I \\
 \alpha_1 &= [n\alpha + g(\cos \theta - X_1 C)]/n' \\
 \beta_1 &= [n\beta + g(\sin \theta - Y_1 C)]/n' \\
 v_1 &= [nv - gZ_1 C]/n'
 \end{aligned}$$

In these,  $\theta$  is the angle of obliqueness of the spherical surface. Its symbol is stipulated as being such that: the radius of the spherical surface to the geometrical light axis (when coaxial, the light axis) is negative when counterclockwise, and positive when clockwise.

227

When calculating the image formation characteristics for noncoaxial systems, this article provides new definitions for the object light axis and the image light axis. These definitions are that (as shown in Fig.10), from the center O of the actual light raster or grating, if one goes out along the geometrical light axis

toward the object area and makes use of the proximate axis light path calculation formula to calculate a light ray, one obtains the radiated light ray AB, that is, the light axis for the object area. Along the object area light axis, it one makes use of the light path tracking formula to trace a light ray, one obtains the radiated light ray CD, that is, the light axis for the image area. The objective of this kind of definition is to guarantee, as much as possible, that light rays that possess the same field of vision and aperture diameters will all be able to go through the actual light raster or grating.

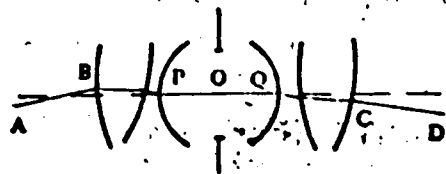


Fig.10 Precise Determination of Light Axes for Object Area and Image Area

#### PRACTICAL DESIGN EXAMPLE

Normally, the optical systems of head up display devices have existing in them the weak points of small fields of vision and the contradiction between high transparency and high reflection. The optical systems of holographic head up display devices overcome these two weaknesses. Making reference to Fig.11, the two record light sources of holographic lenses, O and R, are, respectively, positioned at the entry and exit apertures (pupils). Because of this, the main light ray O going through the entry pupil is, in all cases, capable of making use of strict Prague conditions to defract through the exit pupil R point. As a result of this, one is capable of obtaining very large fields of vision. Due to the fact that the operating wave lengths of holographic lenses and the operating wave lengths of CRTs



are in line with each other, they only possess very high refractive effectiveness on the light waves of fluorescent screens. Moreover, light waves from the outside are almost all not capable of going through holographic lenses without experiencing losses. As a result of this, we have resolved the problem of the contradiction between high transparency and high reflection.

The design of holographic head up display optical systems primarily considers three problems. 1. Exterior form dimensions must satisfy the requirements of the aircraft cockpit space. It determines the aperture diameter passing light through the holographic lens, the angle off the axes, the focal length or distance, and the aperture diameters and focal lengths of compensating lenses. 2. The observation distance of flight personnel or pilots. It principally determines the exit pupil distance of the system. 3. With regard to holographic lens aberrations, what type of formulas to opt for the use of in carrying out compensation.

There are five types of forms or methods for the adjustment or calibration of holographic lens aberrations: reduce the angle off the axis; opt for the use of a curved basic surface holographic lens; opt for the pre-recording of aberrant waves; opt for the use of noncoaxial spherical surface relay lens compensation; and, opt for the use of holographic lens compensation. Among these five types of forms or methods, the first method is affected by the limitations of the aircraft cockpit space requirements. Generally, they are between 35 and 50 degrees. The other four types of methods each has various sorts of advantages and disadvantages. For example, the second and third types of methods are advantageous in reducing the asymmetrical characteristics of image surface obliqueness and aberration distributions. However, the industrial techniques involved in design and manufacture will be somewhat more complicated. Also, in the example of the fifth type of method, the structure is simple, the weight is light, and, speaking in terms of the corresponding design and manufacture, they are relatively easy. However, the capabilities for the calibration of aberrations are limited. In the practical design case in this article, we only opted for the use of the fourth type of method.

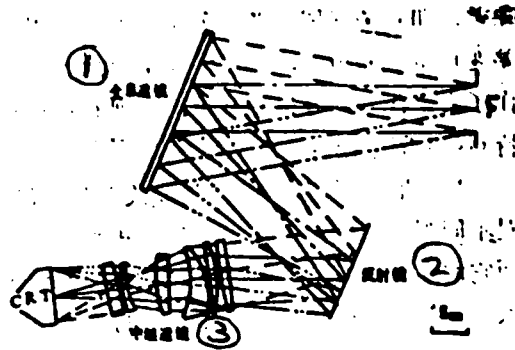


Fig.11 (1) Holographic Lens (2) Reflecting Lens (3) Relay Lenses

Aberration calculations for holographic optical systems are not only a different process from the aberration calculations for normal optical systems. Moreover, there is also a very striking special point which is nothing else than the requirement for a very large exit pupil. Generally, it is a rectangle. This article made a specialized compilation of an "Aberration Calculation Program for Holographic Noncoaxial Spherical Surface Optical Systems." This program possesses simplicity. It has the special feature of flexibility of uses. It is capable of carrying out calculations on image forming light packets or bundles for certain locations and certain aperture diameters in the meridian and arc vector directions for the aperture diameter of entry pupils. Not only is it capable of calculating the aberrations for entire holographic optical systems, it is also capable of independently calculating the aberrations for holographic lenses.

When making calculations, this article selected a universal photographic objective to act as the foundation for relay lenses. In conjunction with this, we opted for reverse direction light path calculations of aberration, that is, on fluorescent screens, we checked for image quality. This article opted for the use of methods

associated with those showing the amount of change in aberrations. Large amounts of detailed analysis and calculations were done on the effects of each variable on aberrations. It was discovered that there are several special points in this way (See Fig.12).

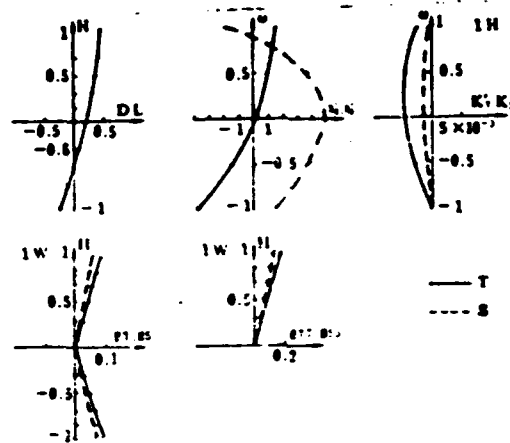


Fig.12 Aberration Curves

228

1. The curvature and thickness of changes, although they are capable of altering aberration values, are, however, still not large influences on the corresponding distributions for aberrations between different fields of vision. However, their changes are relatively large influences on the optical parameters of relay lenses, such as, focal length or distance, entry pupil distance, and other similar parameters. Under relatively stringent requirements for exterior form dimensions, the effects of the calibration of aberrations is also difficult to exert. Because of this, it is not easy to take them and use them as variables to participate in the calibration of aberrations.

2. The primary objects of aberration calibrations are field curvatures, image diffusion, and distortion.

3. Due to the fact that there is no calibration of color aberrations, there is no need to opt for the use of a surface to put them together.

4. Due to the fact that the image obliqueness produced in association with the flat basic surface holographic lens is relatively large, one only uses noncoaxial spherical surface relay lenses, and there is no way to calibrate or correct distortions.

5. As far as image surface obliqueness is concerned, although it is possible to partially calibrate or correct distortions. Its use, however, is very limited. Moreover, it is not advantageous for the calibration or correction of field curvatures and image dispersions.

DISTRIBUTION LIST

DISTRIBUTION DIRECT TO RECIPIENT

ORGANIZATION

MICROFICHE

B085 DIA/RIS-2FI	1
C509 BALLOC509 BALLISTIC RES LAB	1
C510 R&T LABS/AVEADCOM	1
C513 ARRADCOM	1
C535 AVRADCOM/TSARCOM	1
C539 TRASANA	1
Q592 FSIC	4
Q619 MSIC REDSTONE	1
Q008 NTIC	1
Q043 AFMIC-IS	1
E051 HQ USAF/INET	1
E404 AEDC/DOF	1
E408 AFWL	1
E410 ASDTC/IN	1
E411 ASD/FID/TTIA	1
E429 SD/IND	1
P005 DOE/ISA/DDI	1
P050 CIA/OCR/ADD/SD	2
████████████████████	1
1051 AFIT/LDE	1
CCV	1
P090 NSA/CDB	1
2206 FSL	1